Synthesis of Janus and Patchy Particles using Nanogels as Stabilizers in Emulsion Polymerization

Andrea Lotierzo, Brooke W. Longbottom, Wai Hin Lee, and Stefan A. F. Bon*

Department of Chemistry, University of Warwick, Coventry, CV4 7AL, U.K.

ABSTRACT: Polymer nanogels are used as colloidal stabilisers in emulsion polymerization. The nanogels were made by the covalent crosslinking of block copolymer micelles, the macromolecular building blocks of which were synthesized using a combination of catalytic chain transfer emulsion polymerization and reversible addition fragmentation chain-transfer (RAFT) of methacrylate monomers. The use of the nanogels in an emulsion polymerization led to anisotropic Janus and patchy colloids, where a latex particle was decorated by a number of patches on its surface. Control on the particle size and patch density was achieved by tailoring of the reaction conditions, such as varying the amount of nanogels, pH and salt concentration. Overall, the emulsion polymerization process in the presence of nanogels as stabilizers is shown to be a versatile and easily scalable route towards the fabrication of Janus and patchy polymer colloids. **Keywords**: emulsion polymerization, polymer colloids, nanogels, patchy particles, Janus, interface.

The last two decades have seen a surge in efforts to synthesize anisotropic colloidal particles;[1,2] particles with asymmetry in shape and/or chemical composition. Great interest has been shown towards the design and hierarchical assembly of these anisotropic objects, often mimicking biological precision. A wide variety of shapes in colloidal particles have been reported including disks,[3] cubes,[4] cylinders,[5] ellipsoids[6], and more exotic varieties such as "active" matchsticks,[7,8] tetrapods,[9] and even "octopus ocellatus" particles.[10]

Anisotropic colloids with "broken" symmetry are promising candidates as next-generation building-blocks for advanced functional supracolloidal materials.[11,12] The architectural nature of the anisotropic particle is critical to tune the assembly process. The concept of "patchy" particles is often used - particles which have functional sites with a distinct physicochemical characteristic on their surface - as a way to depict directionality and render the desired packing parameter necessary to assemble into a pre-defined supracolloidal structure. The simplest subclass of "patchy" colloids consists of particles having one patch, or protrusion. Such patchy particles are commonly referred to as Janus particles.

Elegant examples of tailored self-assembly in supracolloidal structures using these types of colloids are present in the literature. For instance, Glotzer and coworkers showed *in silico* that colloidal crystals with diamond symmetry, of importance for band gap materials, could be formed using model hard spheres with attractive patches.[13] Sacanna and coworkers reported the assembly of "lock" and "key" colloids which mimic the site specificity of enzymes and receptors to direct supracolloidal assembly.[14,15] Kumacheva *et al.* designed CTAB-coated gold nanorods with polystyrene molecules grafted to both ends that could self-assemble in rings, chains, side-to-side bundles and nanospheres in selective solvents.[16] Granick *et al.* reported that spherical polymer microspheres, made hydrophobic on one hemisphere, could self-assemble in helical-like suprastructures by increasing the ionic strength of the dispersing medium.[17] Instead, when two opposite sides of the microspheres were modified, making "two-sided" Janus particles, the colloidal crystallization into Kagome lattices was observed.[18] Müller, Gröschel *et al.* investigated the use of triblock terpolymers that could form soft patchy particles as building blocks for hierarchical assembly.[19] The formation of supracolloidal polymer chains, spherical clusters and mixed structures laterally decorated by smaller Janus particles was observed.

In recent years, we have witnessed a revolution in the number of approaches to fabricate Janus and patchy particles.[20–22] When we narrow down to the field of polymer science, a number of approaches stand out. Clustering of colloidal objects through collision of particles with either liquid protrusions[23] or hard-soft Janus particles[24]. Assembly of colloidal clusters by using confined solid[25] or droplet templated geometries.[26,27] Heterocoagulation of oppositely charged colloids,[28] or using depletion interaction[14]. Microfluidic strategies including polymerization using droplets,[29] lithography[30], microcontact printing[31] and roll-to-roll printing.[31,32] Other examples include physical deposition after immobilization,[33] surface modification of Pickering stabilizers,[34,35] self-assembly of block-copolymers in multicompartment micelles[36] and so on. Whereas a plethora of synthetic methods is available, a continuous challenge is always to be able to make these materials in scalable amounts using straightforward reproducible synthetic protocols.[21,37]

Here we present a new robust approach to produce patchy and Janus polymer particles in large amounts by modification of a conventional emulsion polymerization process. Patches are positioned onto the surface of spherical latex particles during their synthesis, with appreciable control of the surface density of the patches. The patches are introduced in the form of nanogels (10-30 nm in diameter) which are used as next-generation emulsion polymerization stabilisers. When conventional emulsifiers are used

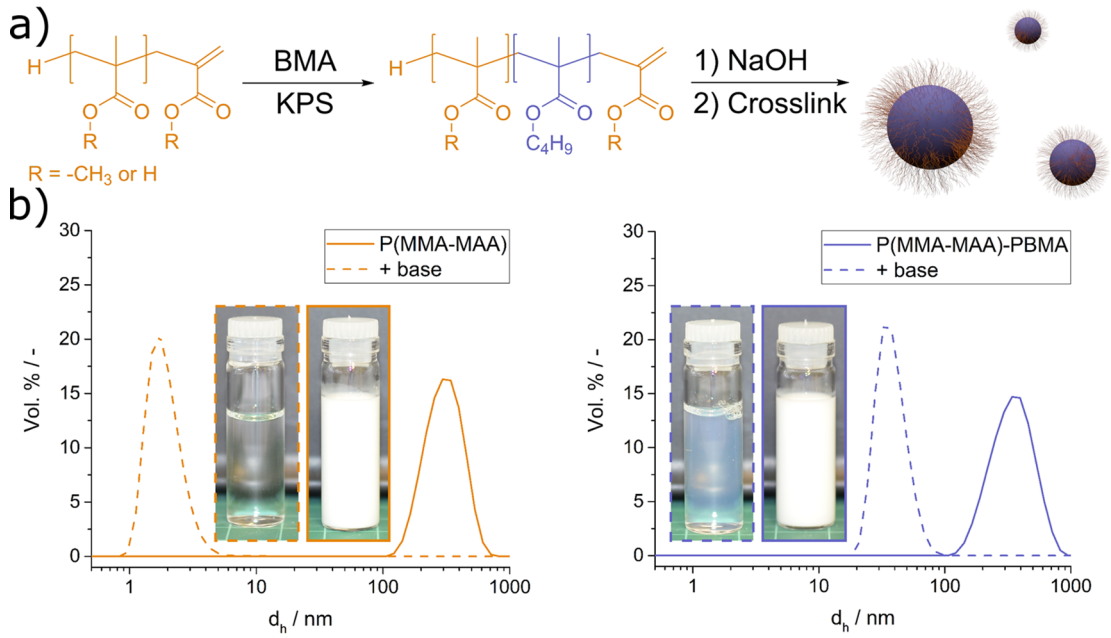

Figure 1. a) Synthesis of crosslinked poly(methyl methacrylate-methacrylic acid)-*block*-poly(*n*-butyl methacrylate) P(MMA-MAA)-PBMA copolymer nanogels. b) Size distribution *via* dynamic light scattering (DLS) before and after addition of base to the polymer latexes.

in emulsion polymerization, they spread out over the entire surface of the latex particle to minimize interfacial tension. Instead, in this work macromolecular surfactants, here with carboxylic acid functionality, were pre-bundled into nanogels to avoid spreading and hereby introducing distinct functional patches. The nanogels we designed were reactive so that during the emulsion polymerization process they strongly locked in place onto the surface of the latex particles.

RESULTS/DISCUSSION

The nanogels adopted in this work were made by core-crosslinking of ω-end unsaturated poly(methyl methacrylate-methacrylic acid)-*block*-poly(*n*-butyl methacrylate) P(MMA-MAA)-PBMA copolymer micelles synthetized *via* sulfur-free reversible addition-fragmentation chain transfer (RAFT) (Scheme 1a).[38–41]

Initially, cobalt-mediated catalytic chain transfer polymerization (CCTP)[42,43] using a mixture of MMA and MAA (1.8:1.0 molar ratio) was carried out as a semi-batch emulsion polymerization process to make polymer latexes in which the particles consist predominantly of ω-end unsaturated poly(methyl methacrylate-*co*-methacrylic acid) P(MMA-MAA) macromonomers. CCTP relies on the use of certain low-spin Co(II) complexes as efficient chain-transfer agents in the polymerization of methacrylate monomers[44] (Scheme S1), and commonly yields α-hydrogen ω-unsaturated telechelic functional polymers.[42] The macromonomers synthesized in this way are an interesting class of compounds as they can operate as macro-RAFT agents in the synthesis of methacrylate block copolymers (Scheme S2), with the added advantage that they do not contain sulfur.[39] These P(MMA-MAA) macromonomer latexes were chain-extended with *n*-butyl methacrylate (BMA) using an analogous protocol as originally reported by Moad and coworkers.[38] Upon addition of base, the diblock copolymer latex particles disassembled to form an aqueous dispersion of copolymer micelles (Figure S2 for cryo-TEM image). In the final synthetic step, these were covalently crosslinked using a trifunctional (meth)acrylate monomer to yield the nanogels (Figure 2). To validate that the polymer chains were indeed bundled into nanogels, dynamic light scattering (DLS) analysis was carried out in MeOH before and after crosslinking (Figure S3). Note that the synthesis of such nanogels cannot be achieved in a controlled fashion by chain-extension of a water soluble polymer *via* dispersion polymerization, or polymerization-induced self-assembly (PISA), as we have recently shown in investigating the use of methacrylate macromonomers in PISA processes.[40]

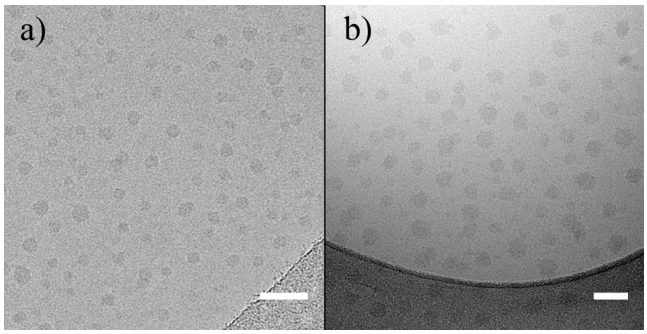

Figure 2. Cryo-TEM images of the nanogels N1 (A) and N2 (B) obtained through crosslinking with trimethylolpropane trimethacrylate. Scale bars: 50 nm.

Two different nanogels were synthetized for this work, N1 and N2 (Table 1). The number average degree of polymerization (*DP*) of the corona hydrophilic block was 17 and 53 respectively, whereas the BMA core hydrophobic block was 10 in both cases. Upon crosslinking, one feature of the nanogels is that they contain two types of carbon-carbon double bonds, reactive towards further polymerization. These are a combination of the ω-end macromonomer vinyl groups and pendant vinyl groups from the trifunctional crosslinker. Their presence was confirmed by ^{1}H-NMR spectroscopy (Figure S4). Interestingly, the nanogels can be stored and used as a dried powder, obtained by freeze-drying, and can be easily re-dispersed in water (Figure S5).

Table 1. Nanogels adopted in this work.

	GPC[a]			SAXS[b]	DLS[c]	
	M_w / kg mol^{-1}	M_n / kg mol^{-1}	Đ / -	d_{SAXS} / nm	d_H / nm	PDI / -
N1	5.6	3.5	1.6	18	30	0.14
N2	11.8	9.0	1.3	23	56	0.04

[a] Gel permeation chromatography (GPC) on the P(MMA-MAA)-PBMA unimers prior to crosslinking; eluent: DMF + 5 mM NH_4BF_4, calibration: PMMA narrow standards. Đ = polymer dispersity.[b] See supporting material for small-angle X-ray scattering (SAXS) data (Table S4, Figures S6 and S7); measured at 10.0 mg/ml, pH 6.0.[c] Measured at 5.0 mg/ml, pH = 8.5.

The nanogels were used as stabilizers in emulsion polymerizations of styrene (Tables S2 and S3). Initially, the reactions were carried out in deionized water at 75°C, pH 8.8, using potassium persulfate (KPS) as initiator and the relative amount of stabiliser was varied. In absence of nanogels, a polystyrene latex of narrow particle size distribution was obtained (d_H = 292 nm, Figure S8). The use of the nanogels had a pronounced effect on the average particle diameter, and its distribution (Figure 3). Upon addition of small amounts, a marked reduction in particle diameter was observed, with a broadening of the particle size distribution upon further increased amounts of nanogels.

This means that the addition of the nanogels had a major effect on the latex particle formation step in the emulsion polymerization process. In a soap-free emulsion polymerization the nucleation of latex particles takes place in the water phase following the so-called homogenous nucleation mechanism (HUFT-theory); the monomer dissolved in the continuous phase polymerizes until it reaches a degree of polymerization, j_{crit}, at which the waterborne oligomer collapses forming a primary particle.[46]

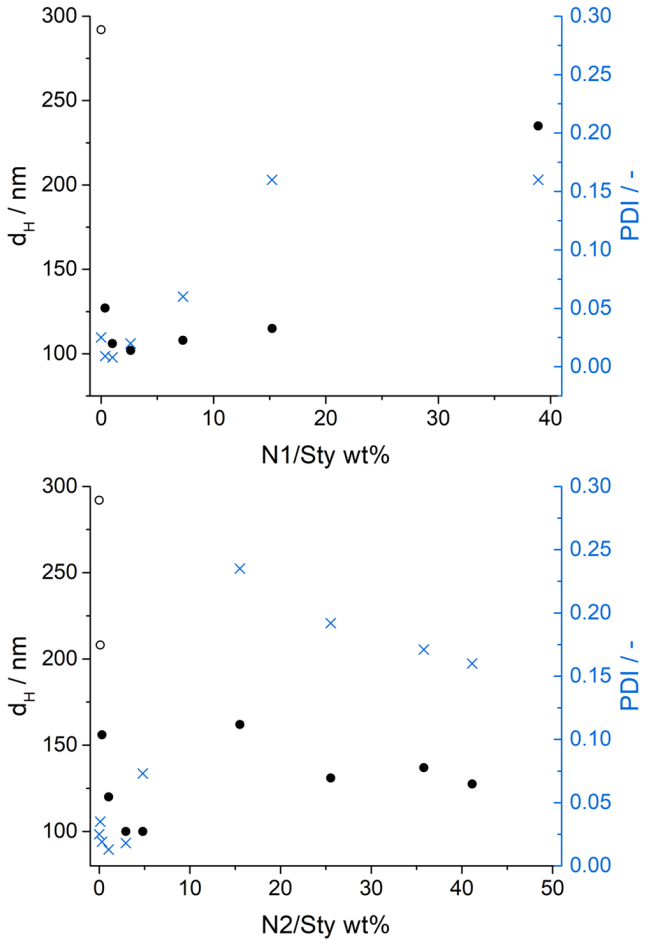

Figure 3. Hydrodynamic diameter (d_H) and polydispersity index (*PDI*) of the final latexes obtained *via* emulsion polymerization of styrene at pH 8.8, carried out in the presence of various amounts of N1 (top) and N2 (bottom), expressed as a weight ratio with respect to styrene. Empty circles: reactions run in the presence of a buffering agent, sodium hydrogen carbonate ($NaHCO_3$), to counteract the pH drop from the KPS decomposition.[45]

In the present case, growing oligomers in the water phase can be captured by the nanogels instead, before j_{crit} is reached, hereby influencing the latex particle nucleation process. This phenomenon resembles the influence on the nucleation of latex particles and their stabilization by inorganic nanoparticles of various morphologies (spheres,[47,48] disks,[49] sheets[50]) and organic Janus particles[51,52] in seeded emulsion polymerization processes. When using inorganic nanoparticles, the morphology of the resulting latex generally is that of a polymer particle with an outer armour of relatively close packed nanoparticles.

Instead, electron microscopy analysis of the polymer latexes made in presence of relatively small amounts of nanogels (< 3.0 wt% wrt to monomer, defined as the weight ratio nanogel/styrene×100) revealed polystyrene particles with no more than one nanogel lobe on the surface (Figures 4A and S9). Therefore, our emulsion polymerization method provides versatile access to polymer Janus particles, char-

acterized by a single nanogel protrusion. Here, we employed nanogels which had carboxylic acid functionality. The Janus polymer particles therefore had a single carboxylic acid functional patch. It is evident that the chemical specificity of the patch can be tuned in the synthesis of the nanogels. It is important that crosslinked colloidal objects are used. Emulsion polymerizations where the non-crosslinked polymer micelles were used instead, resulted in mostly spherical latex particles without distinct patches (Figure S10). Reactions carried out at higher amounts of nanogels produced particles with multiple lobes. However, the average particle diameter, number of lobes, and particle size distribution became erratic (Figures 3 and S11).

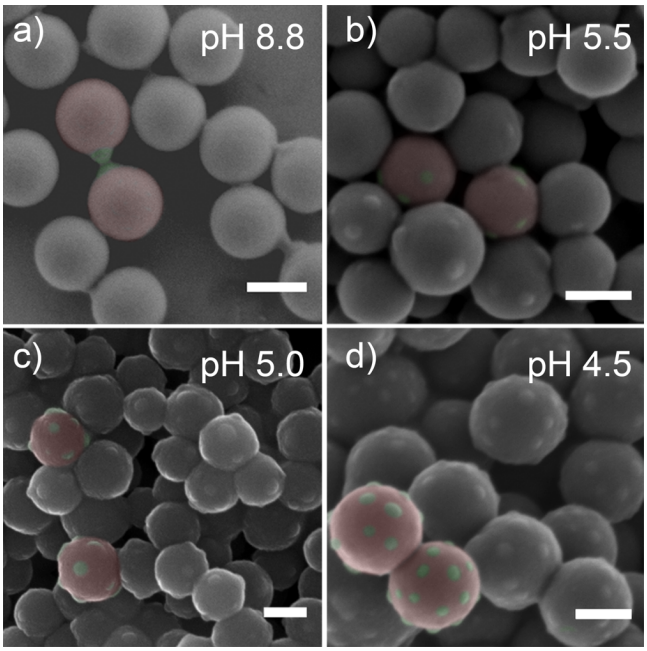

Figure 4. False coloured SEM images of emulsion polymerizations using N1 at 2.8 wt% wrt monomer in which the pH was adjusted to 8.8 (A), 5.5 (B), 5.0 (C) and 4.5 (D) prior to polymerization. Scale bars: 100 nm.

We queried if it was possible to tailor the number of patches, and thus the patch density, without loss of control of the latex particle size distribution. Inspiration and encouragement taken from Pickering (mini)-emulsion polymerizations on the ordering of charged silica nanoparticles onto mini-emulsion droplets[53] and armored polymer latexes[47,54] indicates that it should be possible to control the spacing of particles. By varying the emulsion polymerization conditions with a focus on the electrostatic features of the nanogels, regulation of the number of patches *per* particle, and hence control of patch density was achieved (Figure 4).

The previous set of emulsion polymerizations were conducted at pH 8.8. At this pH the nanogels are colloidally stable due to the presence of deprotonated carboxylic acid groups in their corona. An indicative measure for the relative number of anionic charges present in a nanogel particle is the fraction of ionized carboxylic acid groups, α. Its value is linked directly to pH in the form of a modified Henderson–Hasselbalch equation, taking into account neighbouring electrostatic screening effects.[55,56] At pH 8.8, α approaches a value of 1.0. In this case, at high anionic charge density and potency in electrostatic stabilization, it is plausible that Janus particles are formed upon radical entry into a nanogel "seed" particle, which is swollen with styrene monomer (Figure S12a). As the polymerization proceeds, a polystyrene lobe phase-separates from the crosslinked nanogel core, forming a small anisotropic colloid. The charged nanogel warrants colloidal stability of the Janus particle upon further growth of the poly(styrene) lobe. When decreasing the pH of the nanogel dispersions in water, the loss of surface charge due to the protonation of the carboxylic acid groups, that is the decrease in α, results in a gradual loss of colloidal stability. This behaviour is confirmed when monitoring the average nanogel hydrodynamic diameter (d_H) *versus* pH by DLS (Figures 5 and S13). We can see some reduction in d_H as a result of a lower charge density down to *ca.* pH 5.5. At even lower pH ranges, an increase in size and dispersity was observed as a loss in electrostatic colloidal stability induced particle clustering.

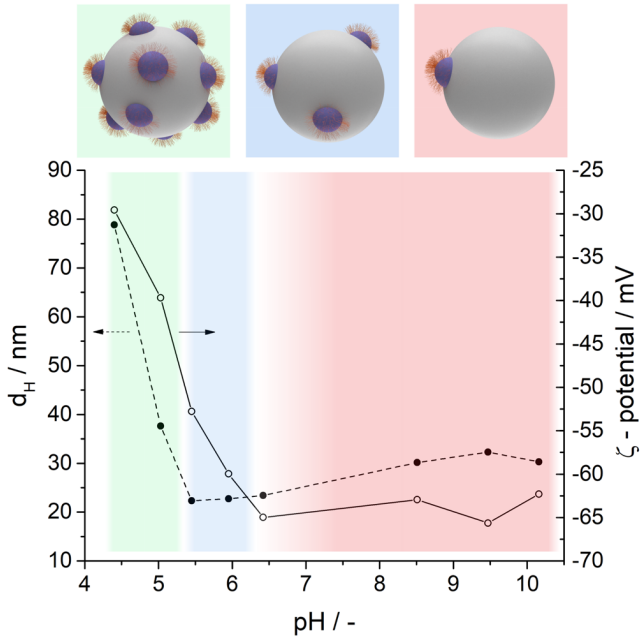

Figure 5. Hydrodynamic diameter (d_H) and ζ-potential variation on N1 as a function of pH. As the double layer is compressed, different particle morphologies can be obtained in the styrene emulsion polymerization.

The ability to control the charge density of the nanogels by variation of pH and their corresponding colloidal stability led to a considerable control of patch density in the polymer colloid synthesis. Emulsion polymerizations conducted at different pH resulted in stable latexes for both N1 and N2 down to about pH 5. At more acidic conditions either coagulation (N2) or latexes with broad particle size distributions (N1) were obtained (Figure S14). A striking example is the emulsion polymerizations using N1 where the pH was set to 5.5 ($\alpha \approx 0.16$-0.22)[55,56] This reaction resulted in the formation of low dispersity patchy particles, where instead of just one, a few nanogel lobes could be seen on the polystyrene surface (Figure 4B). When the pH was further

decreased to 5.0 ($\alpha \approx 0.12$) and 4.5 ($\alpha \approx 0.08$),[55,56] an increasing patch density on the surface was achieved and, as to be expected, overall larger particles were obtained (Figures 4C and 4D).Note that in the case of the reaction run at pH 4.5 some coagulum was formed. This is logical as this reaction operates well below the pKa of the carboxylic acid groups,[56] placing the nanogels at the edge of their colloidal stability. Under these acidic conditions the nanogels can operate as conventional Pickering stabilizers, in other words, they can adhere to the interface of monomer droplets, prior to polymerization. Indeed, small amounts of polymerized monomer droplets with a patchy layer of nanogel particles were observed (Figure S15).

To investigate these observations (Figure 4A-D) in greater detail we carried out in depth image analyses of the SEM data. This to not only get a more accurate view on the size distribution of the Janus and patchy particles, but also to statistically quantify the patch density of particles formed at the four different values of pH. Manual measurements were made in ImageJ on a particle by particle basis in order to assign number of patches to the associated poly(styrene) surface area. The observed number of patches in the SEM images was multiplied by 2 to give n_{patch} to account for patches on the underside masked from our view. To be clear this treatment was applied to all cases including at pH 8.8 whereby all particles in frame (both with one patch and zero patches) were measured and the average observed patch number was doubled. Note that the individual size distributions, that is particles with one patch and particles without an observable patch, were in agreement, validating this approach.

By regulating the pH in emulsion polymerizations, *i.e.* from 8.8 down to 4.5 using N1 nanogels, Figure 6A shows that indeed the particle size of the patchy latexes increases when the pH is lowered (average diameters of 76 ± 5, 117.8 ± 9.1, 133.9 ± 9.2, 165.4 ± 14.2 nm respectively). The increase in particle diameter upon decrease in pH is logical and can be explained as a reduced number of polymerization loci. This is likely a combination of coagulative assembly of growing Janus particles early on in the polymerization process and pre-assembly of nanogels prior to polymerization (Figure S12), as also indicated by Figure 5. The surface area fraction (surface coverage) of patches on the PS surface increased from 3.0 to 16.6% (Figure S16) and the number of patches could be varied from 1 to roughly 18 *per* latex particle (Figure 6B). The role of the nanogels in the formation of patchy particles is to provide electrostatic stability. Whereas at pH 8.8 α approaches a value of 1.0, at pH 5.5, 5.0 and 4.5 α was measured to be *ca.* 0.22-0.16, 0.12 and 0.08 respectively for poly(methacrylic acid).[55,56] This is in agreement to what shown in Figure 5; at pH lower than 6.5 ($\alpha \sim 0.5$)[55] the ζ-potential starts decreasing rapidly with pH. In essence more nanogel patches are required to maintain colloidal stability.

Interestingly, 2D studies of ordering of colloidal particles on liquid-liquid interfaces, showed no dependence in spatial arrangement on pH or salt concentration.[57,58] A comparison with these systems is reasonable as up to high styrene monomer conversion the latex particle core will be swollen, and hence in a liquid state.

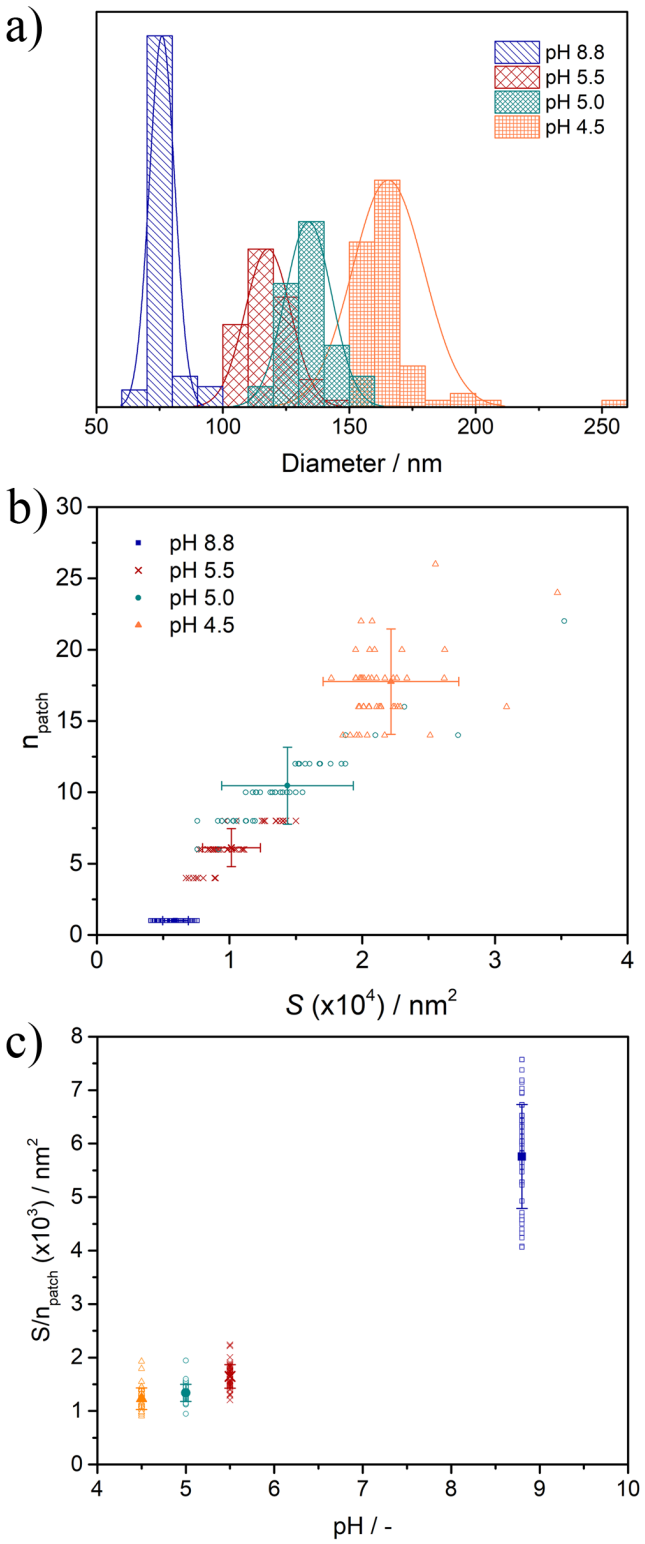

Figure 6. Image analysis of SEM data of latexes made at different pH using N1 nanogels. a) Latex particle diameters showing a normal distribution. b) Number of patches (n_{patch}) on the poly(styrene) surface *versus* total latex surface area (S). In the case of the reaction run at pH 8.8, 51% of the observed particles had a single visible patch on the surface, hence the average was assumed to be one. c) Surface area *per* patch as a function of pH used in the emulsion polymerization. Population averages (filled symbols) are shown for b) and c) with their relative standard deviations.

When we plot the surface area *per* patch (calculated as the ratio of the latex surface area divided by the number of patches present) as a function of pH (Figure 6C), a striking difference emerges. We observe a clear correlation between the spacing of the nanogels on the surface of the polystyrene and, in essence, the degree of ionization of the nanogels.

The experiments where the pH was adjusted to values < 5.5, were not always straightforward, especially when the nanogels N2 were adopted. An elegant way to circumvent the occasional coagulation issues in this lower pH range is decreasing the pH *in-situ* during particle formation. This can be conveniently achieved by increasing the radical flux, or in other words, by adding more initiator to the system while operating at the same temperature. In fact, the decomposition of persulfates in water is known to release hydrogen sulphate ions and to be acid catalysed.[45] In absence of $NaHCO_3$ as buffer and at very low nanogel concentrations, for example 0.11 wt% wrt monomer in Runs 14 and 26 (Tables S2 and S3), the composition of KPS resulted in pH drop *in-situ* to *ca.* 3.4 during the reaction. Most importantly, a blank experiment, with no nanogels and styrene, showed that in the given experimental conditions the pH takes about 14 min to drop to *ca.* 5.0 (Figure S17). This would allow the particles to start growing as small soft peanut-shaped particles that could then self-assemble in a supracolloidal patchy particle when colloidal stability is lost. As a result, near monodisperse patchy particles of bigger sizes could also be targeted at much lower nanogel concentrations than when the pH was lowered before starting the polymerization (Figure S18).

A different strategy to influence patch density is compressing the electrical double layer by the introduction of inert electrolytes, here NaCl (*aq.*). Patchy latexes could be produced up to a NaCl concentration of 10 mM at which the onset of microcoagulation started to be observed (Figure S19). Above this concentration, complete coagulation of the system was observed in both N1 and N2. At 10 mM NaCl a semi-packed shell of nanogels is present at the surface of the polystyrene particles (Figure 7 and S20). Note that at this [NaCl] it is operated at the upper border of colloidal stability and generally bigger and polydisperse polymer colloids were produced than in reactions where less NaCl was used.

CONCLUSIONS

We have shown that emulsion polymerizations carried out in presence of nanogels lead to the formation of Janus or patchy particles. The distinct patches are warranted by the crosslinked nature of the nanogels. One could say that they serve as reactive Pickering stabilizers, or nanogel surfmers. In our work the nanogels were made by covalent crosslinking of block copolymer micelles, the polymer chains of which were made through a combination of catalytic chain transfer emulsion polymerization and reversible addition fragmentation chain-transfer (RAFT) of methacrylate monomers. It is obvious that the nanogels can be made *via* different synthetic routes, the closest analogue being conventional sulphur-based RAFT.

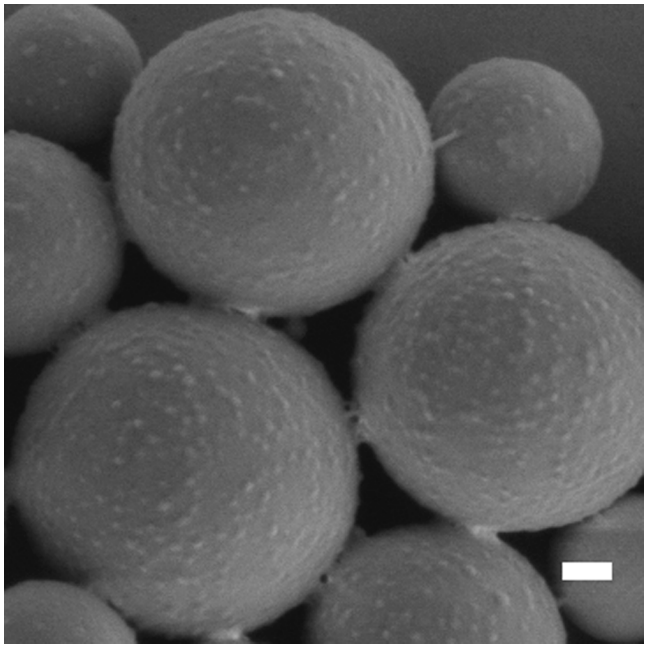

Figure 7. SEM image of the emulsion polymerization of styrene operating at 2.8 wt% N1/styrene and 10 mM NaCl. Scale bar: 100 nm.

A logical extension would be to incorporate chemical functional groups into the nanogels. Without drastic changes in the synthetic protocol, methacrylate monomers carrying poly(ethylene glycol), urea, amino, epoxide, sulfate, vinyl, hydroxy, metal-complexing aceto-acetoxy groups[59] can give specific function to the resulting patchy and Janus particles. The latter in particular could open towards hybrid organic/inorganic patchy particles where the mechanical and catalytic properties of the inorganic components are combined with the film-forming properties and ease of processability of polymeric materials. To conclude, in regard to the reactions carried out at high pH, further injection of monomer in a semi batch process has the potential to allow access to Janus particles with different aspect ratios between lobes.

We hope that the concept we have presented provides a handle in the synthesis of anisotropic polymer colloids, using the convenient, straightforward and industrially scalable synthetic protocols of emulsion polymerization.

METHODS/EXPERIMENTAL

Materials: Methyl methacrylate (MMA) (99%), *n*-butyl methacrylate (BMA) (99%) and styrene (≥ 99%) were purchased from Sigma Aldrich and filtered through activated basic aluminium oxide prior to use to remove the inhibitors. Potassium persulfate (KPS) (99%), 4-4'-azobis(4-cyanovaleric acid) (ACVA) (98%), methacrylic acid (MAA) (99%), trimethylolpropane trimethacrylate (technical grade), trimethylolpropane triacrylate (technical grade), trimethylolpropane ethoxylated triacrylate avg. M_w 428 g/mol (technical grade), sodium dodecyl sulphate (SDS) (≥ 98.5%), sodium hydrogen carbonate ($NaHCO_3$) (≥ 99.7 %), sodium hydroxide (NaOH) (≥ 97%) and d_6-DMSO (99.9 atom % D) were purchased from Sigma Aldrich and used as

received. Bis[(difluoroboryl) dimethylglyoximato]cobalt(II) (CoBF) and bis[(difluoroboryl) diethylglyoximato]cobalt(II) (Et-CoBF) were synthetized according to the literature.[60,61]

Equipment and analysis: ^{1}H-NMR spectra were recorded on freeze-dried polymers on either a Bruker HD-300 or a Bruker HD-400 spectrometer using d_6-DMSO as solvent. The spectra were recorded at 10 wt% polymer in deuterated solvent. Average particle sizes and distributions were measured by dynamic light scattering (DLS) on a Malvern Zetasizer Nano ZS or a Malvern Zetasizer Ultra operating at 25°C and at a detection angle of 173°. ζ-Potential measurement were carried out on the Malvern Zetasizer Ultra at 0.5 wt% in deionized water using disposable folded cuvettes (Malvern). Molecular weights and dispersity values were measured by gel permeation chromatography (GPC) on an Agilent 390-MDS equipped with a Polar Gel Guard and two Polar Gel mixed-D columns operating at 60°C. DMF with 5mM NH_4BF_4 was used as eluent for the GPC analysis and the system was calibrated using narrow molecular weight poly(methyl methacrylate) standards. The GPC samples were prepared at 1-2 mg/ml and were filtrated through a 0.2 μm hydrophilic PTFE filter before injection. Dialysis was performed using semipermeable cellulose tubing (3.5 kDa molecular weight cutoff). Cryogenic Transmission electron microscopy (cryo-TEM) analyses were performed on a Jeol 2200FS TEM. Scanning electron microscopy (SEM) images were collected on a ZEISS Gemini SEM. Samples were diluted in deionized water and casted on a silicon wafer fragment, which had been adhered to an aluminium stab using conductive copper tape. The samples prepared in this way were carbon coated before imaging. Image analysis of SEM data was performed using ImageJ. Size data was obtained by measuring the Feret diameter. To quantify the number of patches per particle and measure associated poly(styrene) surface area per patch, particles were measured one-by-one. The poly(styrene) particle surface area was found by fitting a circle to the particle perimeter. The patches were then counted on the specified particle or measured by fitting an ellipse to the protruding patch. The number of patches per particles was multiplied by 2 to account for those lying on the underside of particle masked from view.

Synthesis of polymer nanogels (N1): The synthesis of the polymeric nanogels was performed in a 250 ml glass reactor equipped with a PTFE coated anchor overhead stirrer and a PTFE coated temperature probe. All the reagents added to the reactors are purged with nitrogen for at least 30 min prior to addition, even when not specified. Step 1: Synthesis of a macromonomer latex via catalytic chain-transfer polymerization (CCTP) in a semi-batch emulsion polymerization process[38,39]: In a typical emulsion polymerization experiment CoBF (8.2 mg) and a MAA:MMA 30:70 v:v mixture (25.0 ml) were purged with nitrogen in separated sealed vials equipped with magnetic bars for 1h. After this time, 22.0 ml of the monomer mixture was added to the vial containing CoBF using a degassed syringe. This mixture was stirred vigorously until complete dissolution of the catalyst; mild ultrasound treatment was used to favour dissolution in this step. Meanwhile, SDS (0.3 g), H_2O (130.0 g), ACVA (0.5 g) were added to a 250 ml reactor and purged with nitrogen for 1 h under vigorous stirring at 300 rpm. Note that ACVA it is not soluble at this stage. After this, the reaction mixture was heated up to 72°C, which rendered ACVA soluble in water. The reaction was started with the addition of 20% by volume of the monomer mixture (the rest was fed at 0.666 ml/min over 24 min, total volume added to the reactor = 20.0 ml) and it was carried out for 1h at 72°C. Next, the system was heated to 82°C and the reaction was left to reach full conversion for one extra hour. Step 2: Chain-extension with n-butyl methacrylate (BMA) via reversible addition-fragmentation chain transfer (RAFT): For the synthesis of N1, 120.0 g of latex were diluted with 38.0 g of water. The reaction was conducted at 85°C while BMA (14.1 ml) and aqueous KPS solution (12.6 ml, 5.6 mg/ml) were fed over 2 h. After feeding, the reaction was allowed to proceed for extra 30 min. Step 3: Latex Solubilization and polymer micelle crosslinking: For the synthesis of N1 nanogels, 133.1 g of BMA chain-extended latex were diluted with 40.0 ml water and 37.3 g of NaOH (1.0 M, aq.) were injected into the system. NaOH was added to a 1.05:1.00 molar ratio wrt MAA. The system was left to equilibrate at 85°C for 30 min and during this time it turned from milky white to translucent blue. After this time, trimethylolpropane trimethacrylate was added to the system (5.9 ml) and aqueous KPS solution (12.6 ml, 5.6 mg/ml) was fed in the system over 5 h. The system was then allowed to fully react overnight. During this stage limited precipitation occurred, which was removed by filtration using hydrophilic PTFE 0.45 μm filters. Final solid content: 11.7 wt%.

Emulsion polymerization using nanogels (N1) as stabilisers: The emulsion polymerizations were carried out in either a 250 ml reactor apparatus as described above, or a sealed 250 ml round bottom flask equipped with an oval stirrer bar. Little difference was found when repeating the same reactions with the two set-ups. In a typical emulsion polymerization experiment (Run 14, Table S3), an aqueous dispersion of nanogels (sample N1, 0.13 g) was diluted with H2O (120.0 g). The pH of the suspension was adjusted to 8.8 using aq. HCl 1.0 M. The reaction mixture was charged in a 250 ml reactor apparatus as previously described and it was purged with nitrogen for 30 min. Next, styrene (12.5 g), which had been previously purged with nitrogen for 30 min, was injected into the reactor using a degassed syringe. The system was heated up to 75°C. The reaction was started upon injection of an aqueous KPS solution (1.0 ml, 19.7 mg/ml) and it was run overnight.

ASSOCIATED CONTENT

Supporting Information. Details on synthetic procedures, additional electron microscopy images and scattering data, ^{1}H-NMR spectra. This material is available free of charge *via* the Internet at http://pubs.acs.org.

The authors declare no competing financial interest.

AUTHOR INFORMATION

Corresponding Author

* s.bon@warwick.ac.uk. www.bonlab.info

ACKNOWLEDGMENT

The Australian paint company Dulux Australia is acknowledged for financial funding (AL). Dr. Saskia Bakker is thanked for helping with Cryo-TEM analysis and acknowledge the University of Warwick Advanced BioImaging Research Technology Platform supported by BBSRC ALERT14 award BB/M01228X/1. Dr. Steven Huband is thanked for the great help in running SAXS analysis. Dr. Ross Jaggers is acknowledged for the false coloring of SEM images.

REFERENCES

(1) Glotzer, S. C.; Solomon, M. J. Anisotropy of Building Blocks and Their Assembly into Complex Structures. *Nat. Mater.* **2007**, *6* , 557–562.

(2) Walther, A.; Müller, A. H. E. Janus Particles: Synthesis, Self-Assembly, Physical Properties, and Applications. *Chem. Rev.* **2013**, *113*, 5194–5261.

(3) Li, Z.; Peng, X. Size/Shape-Controlled Synthesis of Colloidal CdSe Quantum Disks: Ligand and Temperature Effects. *J. Am. Chem. Soc.* **2011**, *133*, 6578–6586.

(4) Gou, L.; Murphy, C. J. Solution-Phase Synthesis of Cu_2O Nanocubes. *Nano Lett.* **2003**, *3*, 231–234.

(5) Kuijk, A.; Van Blaaderen, A.; Imhof, A. Synthesis of Monodisperse, Rodlike Silica Colloids with Tunable Aspect Ratio. *J. Am. Chem. Soc.* **2011**, *133*, 2346–2349.

(6) Ho, C. C.; Keller, A.; Odell, J. A.; Ottewill, R. H. Preparation of Monodisperse Ellipsoidal Polystyrene Particles. *Colloid Polym. Sci.* **1993**, *271*, 469–479.

(7) Longbottom, B. W.; Rochford, L. A.; Beanland, R.; Bon, S. A. F. Mechanistic Insight into the Synthesis of Silica-Based "Matchstick" Colloids. *Langmuir* **2015**, *31*, 9017–9025.

(8) Morgan, A. R.; Dawson, A. B.; McKenzie, H. S.; Skelhon, T. S.; Beanland, R.; Franks, H. P. W.; Bon, S. A. F. Chemotaxis of Catalytic Silica-Manganese Oxide "Matchstick" Particles. *Mater. Horiz.* **2014**, *1*, 65–68.

(9) Talapin, D. V.; Nelson, J. H.; Shevchenko, E. V.; Aloni, S.; Sadtler, B.; Alivisatos, A. P. Seeded Growth of Highly Luminescent CdSe/CdS Nanoheterostructures with Rod and Tetrapod Morphologies. *Nano Lett.* **2007**, *7*, 2951–2959.

(10) Okubo, M.; Kanaida, K.; Matsumoto, T. Production of Anomalously Shaped Carboxylated Polymer Particles by Seeded Emulsion Polymerization. *Colloid Polym. Sci.* **1987**, *265*, 876–881.

(11) Van Blaaderen, A. Materials Science: Colloids Get Complex. *Nature* **2006**, *439*, 545–546.

(12) Glotzer, S. C. Some Assembly Required Space — The Final Frontier. *Science.* **2004**, *306*, 419–420.

(13) Zhang, Z.; Keys, A. S.; Chen, T.; Glotzer, S. C. Self-Assembly of Patchy Particles into Diamond Structures through Molecular Mimicry. *Langmuir* **2005**, *21*, 11547–11551.

(14) Sacanna, S.; Irvine, W. T. M.; Chaikin, P. M.; Pine, D. J. Lock and Key Colloids. *Nature* **2010**, *464*, 575–578.

(15) Wang, Y.; Wang, Y.; Zheng, X.; Yi, G. R.; Sacanna, S.; Pine, D. J.; Weck, M. Three-Dimensional Lock and Key Colloids. *J. Am. Chem. Soc.* **2014**, *136*, 6866–6869.

(16) Nie, Z.; Fava, D.; Kumacheva, E.; Zou, S.; Walker, G. C.; Rubinstein, M. Self-Assembly of Metal-Polymer Analogues of Amphiphilic Triblock Copolymers. *Nat. Mater.* **2007**, *6*, 609–614.

(17) Chen, Q.; Whitmer, J. K.; Jiang, S.; Bae, S. C.; Luijten, E.; Granick, S. Supracolloidal Reaction Kinetics of Janus Spheres. *Science.* **2011**, *331*, 199–202.

(18) Chen, Q.; Bae, S. C.; Granick, S. Directed Self-Assembly of a Colloidal Kagome Lattice. *Nature* **2011**, *469*, 381–384.

(19) Gröschel, A. H.; Walther, A.; Löbling, T. I.; Schacher, F. H.; Schmalz, H.; Müller, A. H. E. Guided Hierarchical Co-Assembly of Soft Patchy Nanoparticles. *Nature* **2013**, *503*, 247–251.

(20) Zhang, J.; Grzybowski, B. A.; Granick, S. Janus Particle Synthesis, Assembly, and Application. *Langmuir* **2017**, *33*, 6964–6977.

(21) Du, J.; O'Reilly, R. K. Anisotropic Particles with Patchy, Multicompartment and Janus Architectures: Preparation and Application. *Chem. Soc. Rev.* **2011**, *40*, 2402–2416.

(22) Pawar, A. B.; Kretzschmar, I. Fabrication, Assembly, and Application of Patchy Particles. *Macromol. Rapid Commun.* **2010**, *31*, 150–168.

(23) Kraft, D. J.; Vlug, W. S.; Van Kats, C. M.; Van Blaaderen, A.; Imhof, A.; Kegel, W. K. Self-Assembly of Colloids with Liquid Protrusions. *J. Am. Chem. Soc.* **2009**, *131*, 1182–1186.

(24) Skelhon, T. S.; Chen, Y.; Bon, S. A. F. Hierarchical Self-Assembly of "hard-Soft" Janus Particles into Colloidal Molecules and Larger Supracolloidal Structures. *Soft Matter* **2014**, *10*, 7730–7735.

(25) Xia, Y.; Yin, Y.; Lu, Y.; McLellan, J. Template-Assisted Self-Assembly of Spherical Colloids into Complex and Controllable Structures. *Adv. Funct. Mater.* **2003**, *13*, 907–918.

(26) Manoharan, V. N.; Elsesser, M. T.; Pine, D. J. Dense Packing and Symmetry in Small Clusters of Microspheres. *Science.* **2003**, *301*, 483–487.

(27) Cho, Y. S.; Yi, G. R.; Lim, J. M.; Kim, S. H.; Manoharan, V. N.; Pine, D. J.; Yang, S. M. Self-Organization of Bidisperse Colloids in Water Droplets. *J. Am. Chem. Soc.* **2005**, *127*, 15968–15975.

(28) Harley, S.; Thompson, D. W.; Vincent, B. The Adsorption of Small Particles onto Larger Particles of Opposite Charge Direct Electron Microscope Studies. *Colloids and Surfaces* **1992**, *62*, 163–176.

(29) Nie, Z.; Li, W.; Seo, M.; Xu, S.; Kumacheva, E. Janus and Ternary Particles Generated by Microfluidic Synthesis: Design, Synthesis, and Self-Assembly. *J. Am. Chem. Soc.* **2006**, *128*, 9408–9412.

(30) Pregibon, D. C.; Toner, M.; Doyle, P. S. Multifunctional Encoded Particles for High-Throughput Biomolecule Analysis. *Science.* **2007**, *315*, 1393–1396.

(31) Kaufmann, T.; Gokmen, M. T.; Wendeln, C.; Schneiders, M.; Rinnen, S.; Arlinghaus, H. F.; Bon, S. A. F.; Du Prez, F. E.; Ravoo, B. J. "Sandwich" Microcontact Printing as a Mild Route towards Monodisperse Janus Particles with Tailored Bifunctionality. *Adv. Mater.* **2011**, *23*, 79–83.

(32) Rolland, J. P.; Maynor, B. W.; Euliss, L. E.; Exner, A. E.; Denison, G. M.; DeSimone, J. M. Direct Fabrication and Harvesting of Monodisperse, Shape-Specific Nanobiomaterials. *J. Am. Chem. Soc.* **2005**, *127*, 10096–10100.

(33) Bae, C.; Moon, J.; Shin, H.; Kim, J.; Sung, M. M. Fabrication of Monodisperse Asymmetric Colloidal Clusters by Using Contact Area Lithography (CAL). *J. Am. Chem. Soc.* **2007**, *129*, 14232–14239.

(34) Jiang, S.; Schultz, M. J.; Chen, Q.; Moore, J. S.; Granick, S. Solvent-Free Synthesis of Janus Colloidal Particles. *Langmuir* **2008**, *24*, 10073–10077.

(35) Ruhland, T. M.; McKenzie, H. S.; Skelhon, T. S.; Bon, S. A. F.; Walther, A.; Müller, A. H. E. Nanoscale Hybrid Silica/Polymer Janus Particles with a Double-Responsive Hemicorona. *Polymer* **2015**, *79*, 299–308.

(36) Gröschel, A. H.; Walther, A.; Löbling, T. I.; Schmelz, J.; Hanisch, A.; Schmalz, H.; Müller, A. H. E. Facile, Solution-Based Synthesis of Soft, Nanoscale Janus Particles with Tunable Janus Balance. *J. Am. Chem. Soc.* **2012**, *134*, 13850–13860.

(37) Jiang, S.; Van Dyk, A.; Maurice, A.; Bohling, J.; Fasano, D.; Brownell, S. Design Colloidal Particle Morphology and Self-Assembly for Coating Applications. *Chem. Soc. Rev.* **2017**, *46*, 3792–3807.

(38) Krstina, J.; Moad, C. L.; Moad, G.; Rizzardo, E.; Berge, C. T.; Fryd, M. A New Form of Controlled Growth Free Radical Polymerization. *Macromol. Symp.* **1996**, *111*, 13–23.

(39) Krstina, J.; Moad, G.; Rizzardo, E.; Winzor, C. L.; Berge, C. T.; Fryd, M. Narrow Polydispersity Block Copolymers by Free-

Radical Polymerization in the Presence of Macromonomers. *Macromolecules* **1995**, *28*, 5381–5385.
(40) Lotierzo, A.; Schofield, R. M.; Bon, S. A. F. Toward Sulfur-Free RAFT Polymerization Induced Self-Assembly. *ACS Macro Lett.* **2017**, *6*, 1438–1443.
(41) Engelis, N. G.; Anastasaki, A.; Nurumbetov, G.; Truong, N. P.; Nikolaou, V.; Shegiwal, A.; Whittaker, M. R.; Davis, T. P.; Haddleton, D. M. Sequence-Controlled Methacrylic Multiblock Copolymers *via* Sulfur-Free RAFT Emulsion Polymerization. *Nat. Chem.* **2016**, *9*, 171–178.
(42) Heuts, J. P. A.; Smeets, N. M. B. Catalytic Chain Transfer and Its Derived Macromonomers. *Polym. Chem.* **2011**, *2*, 2407.
(43) Gridnev, A. A.; Ittel, S. D. Catalytic Chain Transfer in Free-Radical Polymerizations. *Chem. Rev.* **2001**, *101*, 3611–3659.
(44) Haddleton, D. M.; Maloney, D. R.; Suddaby, K. G.; Muir, A. V. G.; Richards, S. N. Catalytic Chain Transfer Polymerisation (CCTP) of Methyl Methacrylate: Effect of Catalyst Structure and Reaction Conditions on Chain Transfer Coefficient. *Macromol. Symp.* **1996**, *111*, 37–46.
(45) Kolthoff, I. M.; Miller, I. K. The Chemistry of Persulfate. I. The Kinetics and Mechanism of the Decomposition of the Persulfate Ion in Aqueous Medium. *J. Am. Chem. Soc.* **1951**, *73*, 3055–3059.
(46) Fitch, R. M. *Polymer Colloids: A Comprehensive Introduction*; 1997.
(47) Lotierzo, A.; Bon, S. A. F. A Mechanistic Investigation of Pickering Emulsion Polymerization. *Polym. Chem.* **2017**, *8*, 5100–5111.
(48) Colver, P. J.; Colard, C. A. L.; Bon, S. A. F. Multilayered Nanocomposite Polymer Colloids Using Emulsion Polymerization Stabilized by Solid Particles. *J. Am. Chem. Soc.* **2008**, *130*, 16850–16851.
(49) Teixeira, R. F. A.; McKenzie, H. S.; Boyd, A. A.; Bon, S. A. F. Pickering Emulsion Polymerization Using Laponite Clay as Stabilizer to Prepare Armored "Soft" Polymer Latexes. *Macromolecules* **2011**, *44*, 7415–7422.
(50) Thickett, S. C.; Zetterlund, P. B. Preparation of Composite Materials by Using Graphene Oxide as a Surfactant in Ab Initio Emulsion Polymerization Systems. *ACS Macro Lett.* **2013**, *2*, 630–634.
(51) Pham, B. T. T.; Such, C. H.; Hawkett, B. S. Synthesis of Polymeric Janus Nanoparticles and Their Application in Surfactant-Free Emulsion Polymerizations. *Polym. Chem.* **2015**, *6*, 426–435.
(52) Walther, A.; Hoffmann, M.; Müller, A. H. E. Emulsion Polymerization Using Janus Particles as Stabilizers. *Angew. Chem. - Int. Ed.* **2008**, *47*, 711–714.
(53) Fortuna, S.; Colard, C. A. L.; Troisi, A.; Bon, S. A. F. Packing Patterns of Silica Nanoparticles on Surfaces of Armored Polystyrene Latex Particles. *Langmuir* **2009**, *25*, 12399–12403.
(54) Colard, C. A. L.; Teixeira, R. F. A.; Bon, S. A. F. Unraveling Mechanistic Events in Solids-Stabilized Emulsion Polymerization by Monitoring the Concentration of Nanoparticles in the Water Phase. *Langmuir* **2010**, *26*, 7915–7921.
(55) Katchalsky, A.; Spitnik, P. Potentiometric Titrations of Polymethacrylic Acid. *J. Polym. Sci.* **1947**, *2*, 432–446.
(56) Kawaguchi, S.; Yekta, A.; Winnik, M. A. Surface Characterization and Dissociation Properties of Carboxylic Acid Core-Shell Latex Particle by Potentiometric and Conductometric Titration. *J. Colloid Interface Sci.* **1995**, *176*, 362–369.
(57) Picard, C.; Garrigue, P.; Tatry, M. C.; Lapeyre, V.; Ravaine, S.; Schmitt, V.; Ravaine, V. Organization of Microgels at the Air-Water Interface under Compression: Role of Electrostatics and Cross-Linking Density. *Langmuir* **2017**, *33*, 7968–7981.
(58) Aveyard, R.; Binks, B. P.; Clint, J. H.; Fletcher, P. D.; Horozov, T. S.; Neumann, B.; Paunov, V. N.; Annesley, J.; Botchway, S. W.; Nees, D.; Parker, A. W.; Ward, A. D.; Burgess A. N. Measurement of Long-Range Repulsive Forces between Charged Particles at an Oil-Water Interface. *Phys. Rev. Lett.* **2002**, *88*, 246102.
(59) Krasia, T.; Schlaad, H. Poly[2-(Acetoacetoxy)Ethyl Methacrylate]-Based Hybrid Micelles. In *Metal-Containing and Metallosupramolecular Polymers and Materials*; 2006; pp 157–167.
(60) Bakac, A.; Brynildson, M. E.; Espenson, J. H. Characterization of the Structure, Properties, and Reactivity of a Cobalt(II) Macrocyclic Complex. *Inorg Chem* **1986**, *25*, 4108–4114.
(61) Bakac, A.; Espenson, J. H. Unimolecular and Bimolecular Homolytic Reactions of Organochromium and Organocobalt Complexes. Kinetics and Equilibria. *J. Am. Chem. Soc.* **1984**, *106*, 5197–5202

SYNOPSIS TOC Polymeric nanogels are used in emulsion polymerization for the tailored synthesis of patchy particles.